



Technical note: Snow Water Equivalence Estimation (SWEE) Algorithm from Snow Depth Time Series Using a Snow Density Model

Noriaki Ohara^{1*}, Siwei He¹, Andrew D. Parsekian², and Thijs Kelleners³

¹Department of Civil and Architectural Engineering, University of Wyoming, 1000 E. University Ave. Laramie, WY 82071

²Department of Geology and Geophysics, University of Wyoming, 1000 E. University Ave. Laramie, WY 82071

³Ecosystem Science and Management, University of Wyoming, 1000 E. University Ave. Laramie, WY 82071

*Corresponding author: noharal@uwyo.edu

Abstract

Snow water equivalence (SWE) is typically computed from snow weight by the SNOTEL system in the US. However, a snow pillow, the main snow weight sensor used by SNOTEL, requires a large, open, flat area (at least 9 square meters) and substantial maintenance costs. This article presents the snow water equivalence estimation (SWEE) algorithm that estimates the SWE evolution merely from continuous snow depth and temperature measurements using common sensors. The key component is a depth-averaged snow density model that is available in the literature, but is underutilized. Here, we demonstrate that the snow density model can estimate mass exchanges (SWE changes due to snowfall, erosion, deposition, and snowmelt) as well as the SWE. The SWEE algorithm can potentially increase the number of snow monitoring locations because snow depth and temperature sensors are considerably more accessible and economical than snow weighing sensor.

1. Introduction

Snow Water Equivalence (SWE) is important for seasonal forecasting of water resource because it is a direct indicator of snow water storage. The basic SWE calculation is snow depth multiplied by snow density. However, in general, it is not straightforward to estimate the season-long evolution of SWE because snow density is difficult to measure directly and without disturbing the snowpack. The snow pillow is a common method to weigh snowpack for SWE computation. This sensor requires a relatively large, open, flat area (3m x 3m, at least), labor-intensive installation, and high maintenance cost. SWE can also be estimated from the difference between passive, natural electromagnetic energy under and above snowpack (e.g. Campbell Scientific, CS725). In contrast, a snow depth measurement is easy to measure continuously using a ranging sensor, even in remote areas since the ranging sensor requires very low power consumption and minimal maintenance. If a simple method to determine snow density is available, SWE could be estimated from the snow depth data without expensive snow pillow or electromagnetic sensors.

Generally, there are two types of approaches for estimating snow density variation. One uses fitted equations, typically a function of time (e.g. Kelly et al., 2003; Jonas et al., 2009; Sturm et al., 2010; Bormann et al., 2014), and the other employs process-based differential equations (e.g. Anderson, 1976).



Kelly et al. (2003) fitted the snow density evolution by a simple logistic curve for processing remote sensing data. Jonas et al. (2009) and Sturm et al. (2010) modeled snow density by the multiple linear regressions and the exponential fitting to snow depth, respectively. Bormann et al. (2014) simply used a linear relationship between mean snow density and the day of year. On the other hand, the snowpack density and its densification rate may be modeled using more detailed empirical but process-based relationships (Kojima, 1967, Mellor, 1975, Anderson, 1976, and Lehning et al., 2002). De Michele et al. (2013) proposed one equation for calculating the bulk snow density, which includes the effects of compaction, metamorphisms, and snow events on snow density. Among others, one of the available models was developed by Kuchment et al. (1983), Motovilov (1986), Anderson (1976), Horne and Kavvas (1997), and completed by Ohara and Kavvas (2006). Although these process-based snow density models are effective under the changing climate, they have not been used for SWE estimation to date. This article proposes a spreadsheet-friendly algorithm to extract more useful information from hourly snow depth and temperature record using the process-based snow density model.

We selected the depth-integrated equation based on the series of the experimental studies on snow metamorphism processes (Bader et al., 1953; Yoshida, 1955; Kojima, 1967; Mellor, 1974, 1975, and 1977), summarized in the supplemental document of this article. The experimental snow density evolution equation was integrated over a snowpack assuming that the snow density at 2/3 of snow thickness from the snow surface can represent the average snow density (von der Heydt, 1992). Accordingly, the depth-averaged snow density evolution may be described by the following ordinary differential equation,

$$\frac{d\rho_s}{dt} = \frac{2}{3\eta_0} D \rho_s e^{-0.04(T_c - T_s)} e^{-k_0 \rho_s} - \frac{(\rho_s - \rho_{ns})\rho_w}{D\rho_{ns}} sn. \quad (1)$$

t = time (hour)
 D = snow depth (cm)
 ρ_s = snowpack density (g/cm³)
 ρ_{ns} = new snow density (g/cm³)
 ρ_w = density of liquid water = 1.0 (g/cm³)
 T_c = critical temperature = 0°C
 T_s = snow surface temperature (°C)
 k_0 = coefficient = 21.0 (cm³/g) (Kojima 1967, Anderson et al. 1976)
 η_0 = viscosity coefficient, a constant at 0 °C = 15.0 ~ 38.0 (cm·hour) (Kojima 1967, Anderson et al. 1976)
 sn = rate of incoming snow (cm/hour)

The exponential term in the right hand side describes the gravitational compaction-snow metamorphism, and the second term expresses the density change created by the new snow deposit. Note that the unit system was restricted in the gram-centimeter-hour system by the original empirical relationships in the literature. Here, we adopt this convenient depth-integrated equation because it sufficiently covers the major snow densification processes as well as being simple.

2. Method

First, the snow density equation, Equation (1), can be rewritten as



$$\frac{d\rho_s}{dt} = G(D, \rho_s, T) + F(D, \rho_s, sn), \quad (2)$$

where

$$G(D, \rho_s, T) = \frac{2}{3\eta_0} D \rho_s e^{0.04T_s} e^{-k_0 \rho_s}, \quad (3)$$

$$F(D, \rho_s, sn) = -\frac{(\rho_s - \rho_{ns})\rho_w}{D\rho_{ns}} sn. \quad (4)$$

The SWE change per unit time, ΔSWE (cm/hour), can be estimated as the difference of Snow Water Equivalences (SWEs) at future time and present time. That is,

$$\Delta SWE = \widehat{SWE}^{i+1} - SWE^i, \quad (5)$$

where the superscript denotes time step, and variable with hat is predicted quantity without SWE deposition or abrasion. The SWE at the present time i can be computed as,

$$SWE^i = D^i \frac{\rho_s^i}{\rho_w}. \quad (6)$$

Similarly, the SWE at the one time step ahead $i+1$ can be computed as,

$$\widehat{SWE}^{i+1} = D^{i+1} \frac{\widehat{\rho}_s^{i+1}}{\rho_w}, \quad (7)$$

where the predicted snow density due only to gravitational compaction may be obtained from Equation (3)

$$\widehat{\rho}_s^{i+1} = \rho_s^i + \Delta t \cdot G(D^i, \rho_s^i, T_s^i). \quad (8)$$

When the change ΔSWE is negative, the snowpack loses its mass by snowmelt, wind erosion, or sublimation. If the change ΔSWE is positive, the snowpack received snowfall or snowdrift. In this case, the depth integrated snow density must be adjusted with new snow density.

$$\begin{cases} \rho_s^{i+1} = \widehat{\rho}_s^{i+1} + \Delta t \cdot F(D^i, \rho_s^i, \Delta SWE) & ; \Delta SWE > 0 \\ \rho_s^{i+1} = \widehat{\rho}_s^{i+1} & ; \Delta SWE \leq 0 \end{cases}. \quad (9)$$

Note that this algorithm requires two assumptions: 1) no snowmelt occurs during snow fall; 2) the density of new snow and drifted snow are the same.

Additionally, snow depth data must be preprocessed by following two steps: 1) removing the measurement oriented abrupt jumps and 2) removing the random noise in the ranging sensor. The latter data process can be performed by either moving average or exponential smoothing filter. In this study, exponential smoothing filter was selected because filtering factor can be easily adjusted even in a spreadsheet. The exponential smoothing filter may be expressed as,

$$D_f^i = \alpha D^i + (1 - \alpha) D_f^{i-1}, \quad (10)$$



106 where D_f^i is the filtered snow depth data at the present time i , and α is the smoothing factor between 0 and
107 1. The smoothing factor may be selected depending on the data error or noise level, and will be discussed
108 in the following section.

109 3. Results and Discussion

110 We applied the SWEE algorithm to data collected at the Brooklyn Lake SNOTEL site (41.3666 N,
111 106.2333W, 3122 m ASL) in the Snowy Range, Medicine Bow National Forest, Wyoming. Figure 1
112 shows the time series of the observed snow depth (upper panel), the model-estimated snow density
113 (second panel), the observed and computed SWE, and the computed SWE fluxes. The snow density
114 model described above was calibrated using three parameters (ρ_{ns} , η_o , and α) for the snow density data
115 by the snow pit survey, denoted in the dot in the second panel of Figure 1, and for the SWE estimates of
116 the SNOTEL. The parameters selected for this demonstrative application were: $\rho_{ns} = 0.18$ (g/cm³), $\eta_o =$
117 21 (cm·hour), $\alpha = 0.1$. The snow temperature was approximated by the hourly air temperature record in
118 this application. The SNOTEL SWE data, denoted by SWE obs., which were computed from the snow
119 depth and snow pillow data by the Natural Resources Conservation Service (NRCS) with the standard
120 procedure, was considered to be “ground truth” in this article.

121 The SWEE algorithm output, denoted by SWE est., was comparable to the SNOTEL SWE, denoted by
122 SWE obs., from the third panel of Figure 1 (Nash–Sutcliffe model efficiency [NSME] = 0.864 and $R^2 =$
123 0.854) (Nash and Sutcliffe, 1970). We find that the timing and magnitude of noticeable changes in SWE
124 is well represented. However, there was some discrepancy in the SWE comparison, including over-
125 prediction of SWE before 18 March 2015 and under-prediction of SWE after 18 March 2015. We pose
126 seven possible reasons for these departures from measured values:

- 127 1. Snow density of newly fallen snow ρ_{ns} is time dependent
- 128 2. Snow erosion and abrasion by wind affect the snow depth observation
- 129 3. Snow pillow measurement brings error into the SWE obs.
- 130 4. Air temperature substitution for snow temperature is questionable
- 131 5. The depth-averaged snow density model is overly simplified
- 132 6. Accuracy of the snow depth measurement is poor
- 133 7. Treatment for the snow depth data is inappropriate

134 There could be different reasons that lead to the discrepancy; however, we found that the most important
135 one may be the new snow density effect (item no.1). Figure 2 shows the sensitivity analysis result for
136 three main model parameters. The NSME coefficient for the SWE was used for the model performance
137 evaluation here. Clearly, new snow density ρ_{ns} is the most sensitive parameter among three parameters
138 (ρ_{ns} , η_o , α). It makes sense that new snow density varies from early winter storms to spring snow events
139 (e.g. Susong et al., 1999). This means that, if accuracies of the all observed data are ensured, it might be
140 possible to analyze the density variation of newly fallen snow using this algorithm in theory. The effect of
141 the air temperature substitution for snow temperature (item no.4) could not be evaluated due to lack of the
142 suitable sensor. On the other hand, the SWE estimation was found to be surprisingly insensitive to the
143 exponential smoothing factor α .



Figure 1 also includes the selected regression model estimates using a power function fitting (Equation (1) in Jonas et al., 2009), multiple linear fittings (Equation (4) in Jonas et al., 2009), and a time adjusted exponential function fitting (Equation (6) in Sturm et al., 2010). The computed statistics, R^2 and NSME, to on the SWE are tabulated in Table 1. It was found that the regression models can capture the mean of the SWE dynamics well while the rapid changes of the snow density after the snow accumulation events could not be expressed. The SWEE algorithm was able to reproduce the overall shape of the SWE time series although the SWE estimation by the SWEE was less accurate than those by the regression models. This is because the SWEE algorithm relies on the predictive snow density change model; therefore, the prediction error of each time step accumulates in the SWE estimate. However, this could lead to the better SWE change estimation (snow accumulation and abrasion) than the regression models during the snow storms because the snow density estimates of the regression models tend to represent the longer period average. More importantly, the SWEE algorithm is based on the process-based snow density model, which is independent from climate, weather, and region.

To further test the performance of the SWEE algorithm, was applied at the Noname (NN) Creek research site (41.3437 N, 106.2121W, 2950 m ASL). The model was recalibrated using a snow density measurement by a snowpit survey on 9 April 2018 near the site, and the parameters were determined as: $\rho_{ns} = 0.22$ (g/cm³), and $\eta_o = 21$ (cm-hour). The site was instrumented with a snow lysimeter, ranging snow depth sensor, and snow surface temperature, but there is no snow pillow at the NN Creek research site. More detailed information regarding this site is available in Pleasants et al. (2017), Thayer et al. (2018), and He et al. (2018). Figure 3 shows the computed SWE change ΔSWE during the snowmelt season of 2018, which includes the lysimetric snowmelt water flux at the bottom of snowpack, denoted in the blue-shaded area. The effect of the smoothing factor α on the SWEE method output can be visualized. When the snow depth data is under-smoothed with $\alpha=0.8$, unrealistic snow gains during the night appeared throughout the snowmelt period, probably due to measurement error. This suggests that the snow ranging sensor has been influenced by local atmospheric conditions affecting ultrasonic wave propagation. On the other hand, the over-smoothed case with $\alpha=0.1$ resulted in continuous snowmelt even during the night time, which is unrealistic, because the lysimetric snow water flux had higher peaks than the SWEE snowmelt rate. Clearly, SWE change estimates, a byproduct of the SWEE algorithm, are highly dependent on the smoothing factor, α , although the SWE estimation was not very sensitive to α . Thus, the smoothing filter is required for snow depth data by a conventional sonic ranging sensor (such as, SR50A-L, Campbell Scientific) in order to eliminate false SWE gains, especially for computing daily-total snowmelt rate.

Additionally, the phase of the peaks can be analyzed using this SWEE change estimate. It is rational to have larger phase difference between the snow lysimeter data and snowmelt (SWE change) in the early snowmelt season because of the thicker snowpack. However, the phase differences were found to be irregular from day to day suggesting that the snow percolation process extremely complicated due to thermal and water flow effects on the snow matrix.

4. Conclusions

This article described the SWEE algorithm that uses the relatively reliable time series data of snow depth and temperature. This method does not rely on snow energy flux computations or empirical snowmelt equation (e.g. temperature index equation), which required significantly more measurements, assumptions,



185 and often model calibrations. As such, the SWEE algorithm has fewer uncertainties than full snow
186 modeling. The small data requirements make this algorithm particularly effective for situations where data
187 is scarce and is a useful tool for quality verification of the existing snow pillow measurements at the
188 SNOTEL sites. The SWE change, which is byproduct of this algorithm, can potentially quantify wind
189 snow erosion, deposition, and sublimation at a very local scale after careful snow density model tuning.
190 To avoid unrealistic SWE exchanges when integrating over a long period, an exponential smoothing filter
191 is recommended to correct the long term mass balance estimates. However, the choice of the parameter
192 of the exponential smoothing filter must depend on the purpose of the analysis. We recommend additional
193 snow surveys (e.g. snow pit, snow course) that provide model calibration opportunities and some
194 confidence in the SWE and SWE change estimations.

195 Lastly, approximation of snow surface temperature by air temperature may not be suitable depending on
196 the energy flux fraction. Thus, this study suggests that snow surface temperature be added to any snow
197 monitoring system because it is more appropriate than air temperature for SWE estimation.

198 **Acknowledgements**

199 This study was supported by the National Science Foundation EPS-1208909. The spreadsheets for the
200 SWEE algorithm computations are available as supplementary document.

201 **References**

- 202 Anderson, E. A.: A Point Energy and Mass Balance Model of a Snow Cover. Silver Spring, Md Us.
203 National Oceanic and Atmospheric Administration (NOAA), Technical Report NWS, 19, 1976
- 204 Bader, H., Neher, J., Eckel, O., Thams, C., Haefeli, R., and Bucher, E.: Der schnee und seine
205 metamorphose. Kommissionsverlag Kümmerly & Frey, Druck von Aschmann & Scheller a.-g.,
206 Zürich, English Translation 14, Snow and its Metamorphism, Snow, Ice and Permafrost Research
207 Establishment, US ACE, 313 pp., 1939.
- 208 Bormann, K. J., Evans, J. P., and McCabe, M. F.: Constraining snowmelt in a temperature-index model
209 using simulated snow densities, *Journal of Hydrology*, 517, 652–667.
210 <https://doi.org/https://doi.org/10.1016/j.jhydrol.2014.05.073>, 2014.
- 211 De Michele, C., Avanzi, F., Ghezzi, A., and Jommi, C.: Investigating the dynamics of bulk snow density
212 in dry and wet conditions using a one-dimensional model, *The Cryosphere*, 7(2), 433.
213 <https://doi.org/http://dx.doi.org/10.5194/tc-7-433-2013>, 2013.
- 214 He, S., Ohara, N., and Miller, S. N.: Understanding sub-grid variability of snow depth at 1 km scale using
215 Lidar measurements, *Hydrologic Processes*, under review, 2018.
- 216 Horne, F. E., and Kavvas, M. L.: Physics of the spatially averaged snowmelt process, *Journal of*
217 *Hydrology*, 191(1-4), 179-207, 1997.
- 218 Jonas, T., Marty, C., & Magnusson, J.: Estimating the snow water equivalent from snow depth
219 measurements in the Swiss Alps, *Journal of Hydrology*, 378(1-2), 161-167, 2009.



- 220 Kelly, R. E., Chang, A. T., Tsang, L., and Foster, J. L.: A prototype AMSR-E global snow area and snow
221 depth algorithm, *IEEE Transactions on Geoscience and Remote Sensing*, 41(2), 230–242,
222 <https://doi.org/10.1109/TGRS.2003.809118>, 2003.
- 223 Kojima, K.: Densification of seasonal snow cover, *Physics of Snow and Ice: Proceedings*, 1(2), 929–952,
224 1967.
- 225 Kuchment, L. S., Demidov, V. N., and Motovilov, Y. G.: River runoff formation (physically
226 based models), Nauka, Moscow, 1983.
- 227 Lehning, M., Bartelt, P., Brown, B., Fierz, C., and Satyawali, P.: A physical SNOWPACK model for the
228 Swiss avalanche warning: Part II. Snow microstructure, *Cold regions science and technology*, 35(3),
229 147–167, 2002.
- 230 Mellor, M.: A review of basic snow mechanics. US Army Cold Regions Research and Engineering
231 Laboratory, 1974.
- 232 Mellor, M.: A review of basic snow mechanics, *IAHS-AISH Publ.*, No. 114, 251–291, 1975.
- 233 Mellor, M.: Engineering properties of snow, *Journal of Glaciology*, 19(81), 15–66, 1977.
- 234 Motovilov, Y. G.: A model of snow cover formation and snowmelt processes, *Int Assoc Hydrol Sci*, (155),
235 47–57, 1986.
- 236 Nash, J. E., and Sutcliffe, J. V.: River flow forecasting through conceptual models part I—A discussion of
237 principles, *Journal of hydrology*, 10(3), 282–290, 1970.
- 238 Ohara, N., and Kavvas, M. L.: Field observations and numerical model experiments for the snowmelt
239 process at a field site, *Advances in water resources*, 29(2), 194–211, 2006.
- 240 Pleasants, M.S., Kelleners, T., and Ohara, N.: Analysis of snowpack dynamics during the spring melt
241 season using point measurements and numerical modeling, *Hydrological Processes*, 31(25), 4568–
242 4585, 2017.
- 243 Sturm, M., Taras, B., Liston, G. E., Derksen, C., Jonas, T., & Lea, J.: Estimating snow water equivalent
244 using snow depth data and climate classes, *Journal of Hydrometeorology*, 11(6), 1380–1394, 2010.
- 245 Susong, D., Marks, D., and Garen, D.: Methods for developing time-series climate surfaces to drive
246 topographically distributed energy-and water-balance models, *Hydrological Processes*, 13(12–13),
247 2003–2021, 1999.
- 248 Thayer, D., Parsekian A. D., Hyde, K., Speckman, H., Beverly, D., Ewers, B., Covalt, M., Fantello, N.,
249 Kelleners, T., Ohara, N., and Rogers, T.: Geophysical Measurements to Determine the Hydrologic
250 Partitioning of Snowmelt on a Snow-Dominated Subalpine Hillslope. *Water Resources Research*, in
251 print, 2018.
- 252 Von der Heydt, L.: Application of a point energy balance model of a snow cover, U. of Calif., Davis,
253 1992.



254 Yoshida, Z.: Physical studies on deposited snow, Hokkaido University Institute of Low Temperature
255 Science, 1955.

256



257 **Table 1 – Statistics of the model fittings with respect to SWE at the Brooklyn Lake SNOTEL site during the**
258 **water year 2015**

Snow density model	R²	NSME	Note
SWEE (this study)	0.864	0.816	Process-based snow density model
Jonas et al. 2009, Eqn.(1)	0.726	0.718	Regression to snow depth with a power function with a single parameter
Jonas et al. 2009, Eqn.(4)	0.937	0.933	Regression to snow depth with a linear function with monthly parameters
Sturm et al. 2010, Eqn.(6)	0.911	0.859	Regression to snow depth with an exponential function with day-of-year adjustment

259

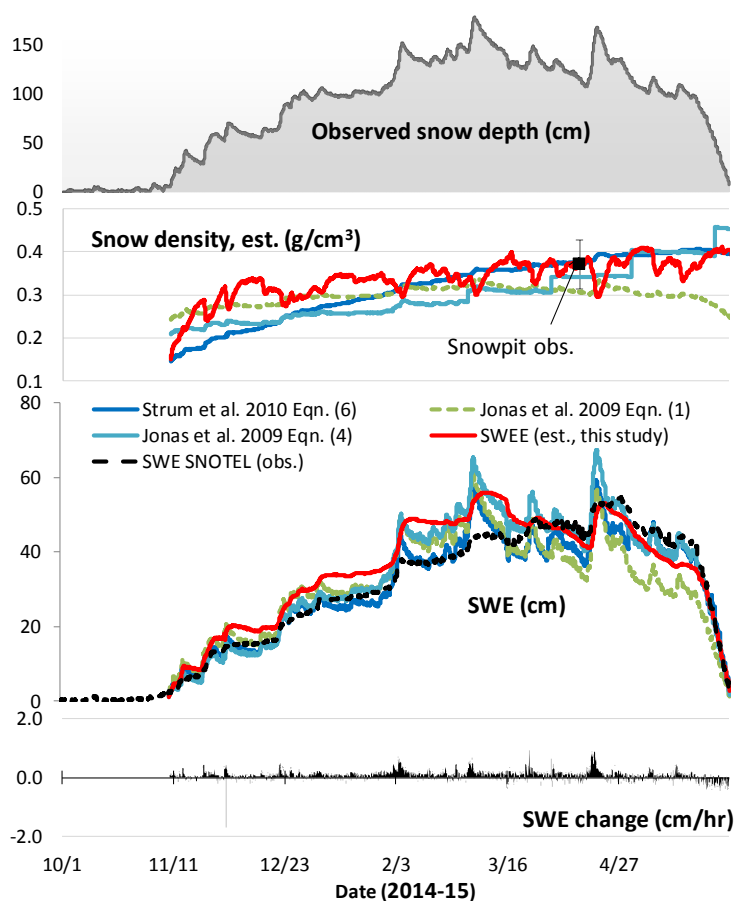


Figure 1 - SWEE application example at the Brooklyn Lake SNOTEL site during the water year 2015. Three regression models (Strum et al., 2010; Jonas et al., 2009) are included in the snow density and SWE graphs in the middle two panels.

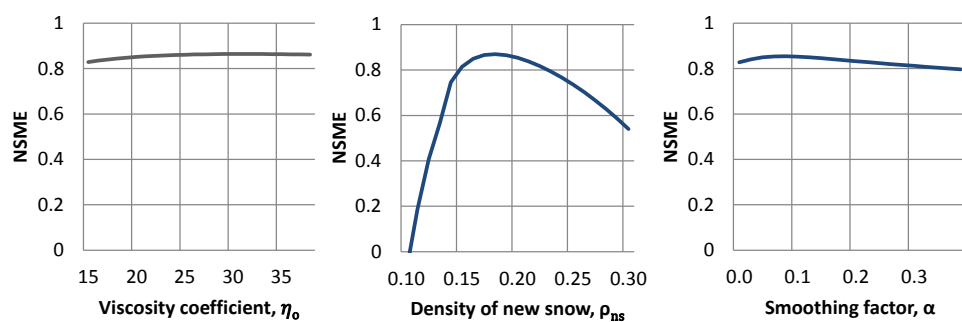


Figure 2 - Sensitivity analysis of the snow density model for SWE estimation

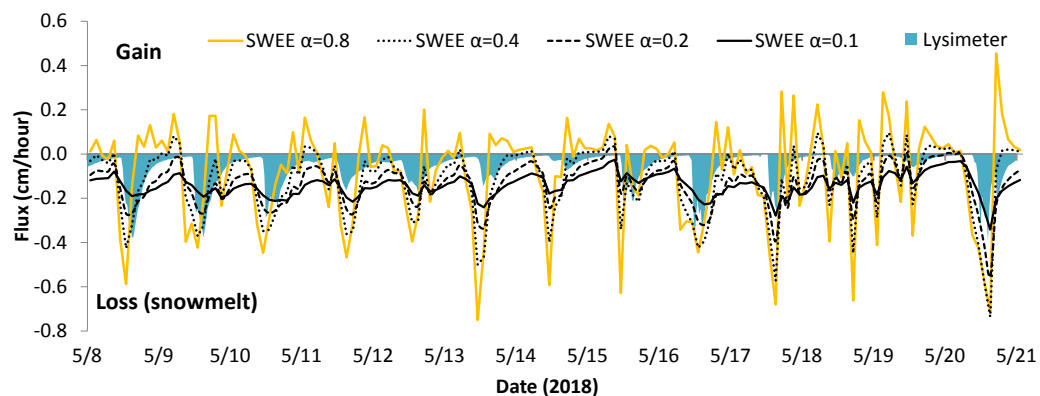


Figure 3 - SWE change computed by the SWEE algorithm and corresponding the lysimetric snowmelt water flux at the bottom of the snowpack in the NN research site